Electronic Supplementary Material (ESI) for ChemComm.
This journal is © The Royal Society of Chemistry 2021

Electronic Supplementary Information

Oxygen-coordinated molybdenum single atom catalyst for efficient electrosynthesis of ammonia

Jing Geng,[†ab] Shengbo Zhang,[†a] Hui Xu,[ab] Guozhong Wang,[a] and Haimin Zhang*[a]

[a] Key laboratory of Materials Physics, Centre for Environmental and Energy Nanomaterials, Anhui Key Laboratory of Nanomaterials and Nanotechnology, CAS Center for Excellence in Nanoscience, Institute of Solid State Physics, HFIPS, Chinese Academy of Science, Hefei 230031, China. E-mail: zhanghm@issp.ac.cn

[b] University of Science and Technology of China, Hefei 230026, China.

1. Experimental

Materials: Sodium molybdate dehydrate was purchased from Aladdin Ltd. (Shanghai, China). Hydrogen peroxide and sulphuric acid were purchased from Sinopharm Chemical Reagent Co., Ltd. (China). Activated carbon was bought from Fuzhou Yihuan Carbon Co., Ltd. (China). The water used throughout all experiments was purified through a Millipore system. All chemicals were used as received without further purification.

Synthesis of Mo-SAs/AC: 2.0 mg activated carbon (AC) was dispersed into 200 mL piranha solution. The mixture was stirred at room temperature for 6 h, followed by filtration and drying. The dried products were then dispersed into 400mL of 20 mmol Mo^{6+} solution. The solution was stirred for 12 hours at room temperature, followed by centrifugation and drying. Mo-NPs/AC was formed. Next, 40 mL of H_2SO_4 was added into 80 mL of deionized water, then Mo-NPs/AC was immersed, and stirred for 6 h at 120 ^oC. After being cooled naturally to room temperature, the product was centrifuged and dried. To obtain Mo-SAs/AC, the precursor powder was then calcinated at 600°C for 2 h with heating rate of 2 $^oC\ min^{-1}$ in N_2 flow.

Characterization: The crystalline structures of samples were identified by the X-ray diffraction analysis (XRD, Philips X'pert PRO) using Nifiltered monochromatic CuKa radiation (λKα1 = 1.5418 Å) at 40 kV and 40 mA. Transmission electron microscope (TEM) images of samples were obtained using JEMARM 200F operating at an accelerating voltage of 200 kV. High-resolution transmission electron microscope (HRTEM), scanning TEM images (STEM) and elemental mapping images of samples were obtained on a JEOL-2010 transmission electron microscope. Furthermore, the spherical aberration corrected (Cs-corrected) high angle annular dark field scanning transmission electron microscopy (HAADF-STEM) and the energy-dispersive X-ray (EDX) mapping experiments were performed using FEI Titan G2 microscope equipped with a Super-X detector at 300 kV. X-ray photoelectron spectroscopy (XPS) analysis was performed on an ESCALAB 250 X-ray photoelectron spectrometer (Thermo, America) equipped with Al Kα1, 2 monochromatized radiations at 1486.6 eV X-ray source. Nitrogen adsorption-desorption isotherms were measured using an automated gas sorption analyzer (Autosorb-iQ-Cx). XAFS spectra were obtained at the 1W1B station in the BSRF (Beijing Synchrotron Radiation Facility, People's Republic of China) operated at 2.5 GeV with a maximum current of 250 mA. XAS measurements at the Mo K-edge were performed in fluorescence mode using a Lytle detector. All samples were

pelletized as disks of 13 mm diameter with 1 mm thickness using graphite powder as a binder. The ^{15}N isotopic labeling experiments were conducted using $^{15}N_2$ as the feeding gas (99% enrichment of ^{15}N in $^{15}N_2$, Supplied by Hefei Ninte Gas Management Co., LTD). The ^{1}H NMR (nuclear magnetic resonance) spectra were obtained using superconducting Fourier transform nuclear magnetic resonance spectrometer (Bruker Avance-400). $(^{15}NH_4)_2SO_4$ as reference samples was dissolved in 0.1 M Na_2SO_4 solution (D_2O/H_2O mixed solution, V_{D2O}:V_{H2O} =1:4) for ^{1}H NMR measurements, and the electrolyte obtained from $^{15}N_2$-saturated 0.1 M Na_2SO_4 solution with the reaction time of 2 h and concentration time of 12 h at 80 °C (D_2O/electrolyte mixed solution, V_{D2O}:$V_{electrolyte}$ =1:4) for ^{1}H NMR measurements.

Electrochemical measurements. All electrochemical measurements were performed on a CHI 660E electrochemical workstation (CH Instrumental Corporation, Shanghai, China) using a two-compartment cell, which was separated by Nafion 117 proton exchange membrane. Nafion membrane (Nafion 117) was protonated prior to the NRR experiments. First, the Nafion 117 was boiled in deionized water for 30 min, then in H_2O_2 for 1 h and subsequently in deionized water for another 1 h, then in 0.5 M H_2SO_4 for 2 h, and finally in deionized water for 5 h, all of which were treated at 80 °C. Different catalyst inks were prepared by dispersing 0.5 mg sample into 100 μL of ethanol and 100 μL of water and 20 μL of Nafion (5 wt.%) under ultrasonic, and were then dropped on the commercial glassy carbon (GC) plate (1.0×1.0 cm^2) as the working electrode. A Ag/AgCl electrode was used as the reference electrode and a Pt wire was used as the counter electrode. The polarization curves were measured with a scan rate of 5.0 mV s^{-1} at room temperature and all polarization curves were obtained at the steady-state ones after several cycles. For N_2 reduction reaction (NRR) experiments, the potentiostatic test was conducted for 2 h in N_2-saturated 0.1 M Na_2SO_4 solution (30 mL) by continuously supplying N_2 into the electrolyte under ambient conditions. In this work, all measured potentials (*vs.* Ag/AgCl) were transformed into the potentials *vs.* reversible hydrogen electrode (RHE) based on the following equation:

$$E_{\mathrm{RHE}} = E_{\mathrm{Ag/AgCl}} + 0.059\mathrm{pH} + E^{\circ}_{\mathrm{Ag/AgCl}}$$

Determination of ammonia. Concentration of the produced ammonia was spectrophotometrically detected by the indophenol blue method. In detail，5 mL of sample was taken, and then diluted with 5 mL of deionized water. Subsequently, 100 μL of oxidizing solution (sodium hypochlorite

(ρCl=4~4.9) and 0.75 M sodium hydroxide), 500 μL of colouring solution (0.4 M sodium salicylate and 0.32 M sodium hydroxide) and 100 μL of catalyst solution (0.1g $Na_2[Fe(CN)_5NO]\cdot 2H_2O$ diluted to 10 mL with deionized water) were added respectively to the measured sample solution. After the placement of 1 h at room temperature, the absorbance measurements were performed at wavelength of 697.5 nm. The obtained calibration curve was used to calculate the ammonia concentration.

Determination of hydrazine. The hydrazine present in the electrolyte was estimated by the method of Watt and Chrisp. A mixture of para-(dimethylamino) benzaldehyde (5.99 g), HCI (concentrated, 30 mL) and ethanol (300 mL) was used as a color reagent. In detail, 2 mL of sample was taken, and then diluted with 8 mL 0.1 M HCl solution. Subsequently, 5.0 mL of the prepared color reagent was added to the above sample solution. Subsequently, the absorbance measurements were performed after the placement of 20 min at wavelength of 455 nm. The obtained calibration curve (Fig. S8) was used to calculate the $N_2H_4\cdot H_2O$ concentration.

Calculations of NH_3 yield rate and Faradaic efficiency.

The equation of NH_3 yield rate:

$$R(\mathrm{NH_3})(\mu g\ h^{-1}\ mg_{Mo}^{-1}) = \frac{C(\mathrm{NH_4^+ - N})(\mu g\ mL^{-1}) \times V(mL) \times 17}{t(h) \times m(mg) \times 0.18\% \times 14}$$

where $R(NH_3)$ is the ammonia yield rate; C (NH_4^+-N) is the measured mass concentration of NH_4^+-N; V is the electrolyte solution volume; t is the reaction time; 14 is the molar mass of NH_4^+-N atom; 17 is the molar mass of NH_3 molecules; m was the loading mass of catalysts; and the content of Mo in Mo SAs/AC is 0.18 wt.%.

The equation of Faradaic efficiency:

$$FE(\mathrm{NH_3})(\%) = \frac{3 \times n(\mathrm{NH_3})(mol) \times F}{Q} \times 100\%$$

where F is the Faradaic constant (96485.34); Q is the total charge during the NRR.

2. Additional Tables and Figures

Table S1. Performances of the reported single atom electrocatalysts and Mo-SAs/AC in this work.

References	Catalyst	Conditions	NH_3 Production Rate	Faradaic Efficiency (%)	Detection method
			Single-Atom Electrocatalysts		
1	Au SAs/C_3N_4	0.005 M H_2SO_4	1305 μg h^{-1} mg_{Au}^{-1} (-0.2 V *vs.* RHE)	11.1	Indophenol method
2	Ru SAs/N-C	0.05 M H_2SO_4	120.9 μg h^{-1} mg_{cat}^{-1} (-0.2 V vs. RHE)	29.6	Indophenol method
3	Ru@ZrO_2/NC	0.1 M HCl	3665 μg h^{-1} mg_{Ru}^{-1} (-0.21 V vs. RHE)	21	Indophenol method
4	SA-Mo/NPC	0.1 M KOH	34.0 ± 3.6 μg h^{-1} mg_{cat}^{-1} (-0.3 V vs. RHE)	14.6 ± 1.6	Indophenol method
5	Fe_{SA}-N-C	0.1 M KOH	7.48 μg h^{-1} mg_{cat}^{-1} (0 V vs. RHE)	56.55	Indophenol method
6	ISAS-Fe-N-C	0.1 M PBS	62.9 ± 2.7 μg h^{-1} mg_{cat}^{-1} (-0.4 V vs. RHE)	18.6 ± 0.8	Indophenol method
7	Mo^0/GDY	0.1 M Na_2SO_4	145.4 μg h^{-1} mg_{cat}^{-1} (-1.2 V *vs.* SCE)	21	Indophenol method
8	NC-Cu SA	0.1 M KOH	53.3 μg h^{-1} mg_{cat}^{-1} (-0.35 V vs. RHE)	13.8	Indophenol method
		0.1 M HCl	49.3 μg h^{-1} mg_{cat}^{-1} (-0.3 V vs. RHE)	11.7	
9	Fe_1-N-C	0.1M HCl	1.56 × 10^{-11} mol cm^{-2} s^{-1} (-0.05 V *vs.* RHE)	4.51	Indophenol method
10	Co SA/NPC	0.05M Na_2SO_4	0.86 μmol cm^{-2} h^{-1} (-0.2 V vs. RHE)	10.5	Indophenol method
11	Ru SAs/g-C_3N_4	0.5 M NaOH	23.0 μg h^{-1} mg_{cat}^{-1} (-0.05 V vs. RHE)	8.3	Indophenol method
12	Fe-SAs/LCC/GC	0.1 M KOH	307.7 μg h^{-1} $mg_{cat.}^{-1}$ (-0.15 V *vs.* RHE)	51.0	Indophenol method

13	Co-SAs/NC-L	0.005 M H_2SO_4	16.9 μg h^{-1} mg_{cat}^{-1} (-0.25 V *vs.* RHE)	27.4 (-0.15 V *vs.* RHE)	Indophenol method
14	Fe-SnO_2	0.1 M HCl	82.7 μg h^{-1} mg_{cat}^{-1} (-0.3 V *vs.* RHE)	20.4	Indophenol method
15	SA Ru-Mo_2CT_x	0.5 M K_2SO_4	40.57 μg h^{-1} mg_{cat}^{-1} (-0.3 V *vs.* RHE)	25.77	Indophenol method
16	Fe-MoS_2	0.1 M KCl	97.5 ± 6 μg h^{-1} cm^{-2} (-0.2 V vs. RHE)	31.6 ± 2	Indophenol method
17	MoSAs-Mo_2C/NCNTs	0.005 M H_2SO_4	16.1 μg h^{-1} mg_{cat}^{-1} (-0.25 V vs. RHE)	7.1	Indophenol method
18	Fe-MoS_2	0.5 M K_2SO_4	8.63 μg h^{-1} mg_{cat}^{-1} (-0.3 V vs. RHE)	18.8	Indophenol method
19	SA-Ag/NC	0.1 M HCl	270.9 μg h^{-1} mg_{cat}^{-1} (-0.65 V *vs.* RHE)	21.9 (-0.60 V *vs.* RHE)	Indophenol method
20	Pd-GDY	0.1 M Na_2SO_4	4.45 ± 0.3 mg h^{-1} mg_{Pd}^{-1} (-0.16 V *vs.* RHE)	31.62 ± 1.06	Indophenol method
21	Mn-O_3N_1/PC	0.1 M HCl	66.41± 4.05 mg h^{-1} mg_{cat}^{-1} (-0.35 V *vs.* RHE)	8.91 ± 0.82	Indophenol method
22	Ni-N_x-C	0.1 M KOH	81 ± 3 μg h^{-1} cm^{-2} (-0.3 V *vs.* RHE)	12.4 ± 1.5	Indophenol method
23	Y_1/NC	0.1 M HCl	23.2 μg h^{-1} cm^{-2} (-0.1 V *vs.* RHE)	12.1	Indophenol method
	Sc_1/NC		20.4 μg h^{-1} cm^{-2} (-0.1 V *vs.* RHE)	11.2	
This work	Mo-SAs/AC	0.1 M Na_2SO_4	2.55 ± 0.31 mg h^{-1} mg_{Mo}^{-1} (-0.4 V vs. RHE)	57.54 ± 6.98	Indophenol method

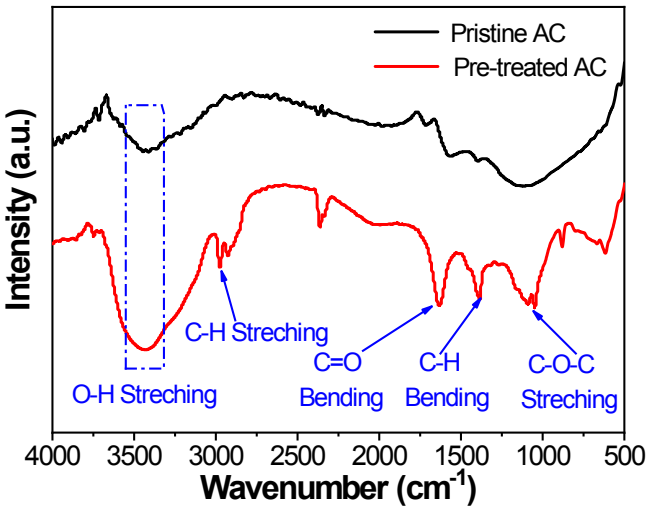

Fig. S1 FT-IR spectra of pristine AC and pre-treated AC.

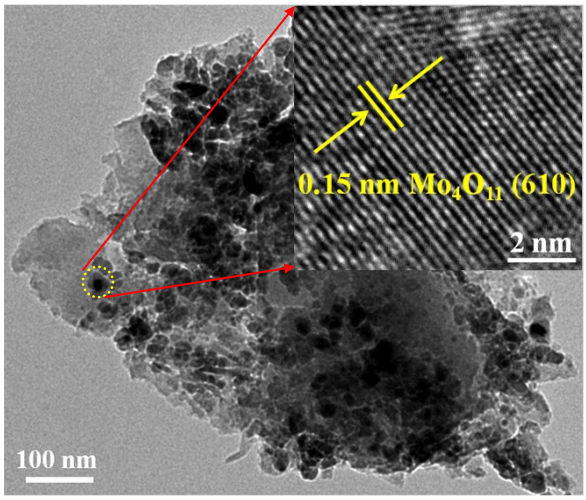

Fig. S2 TEM image of Mo NPs/AC.

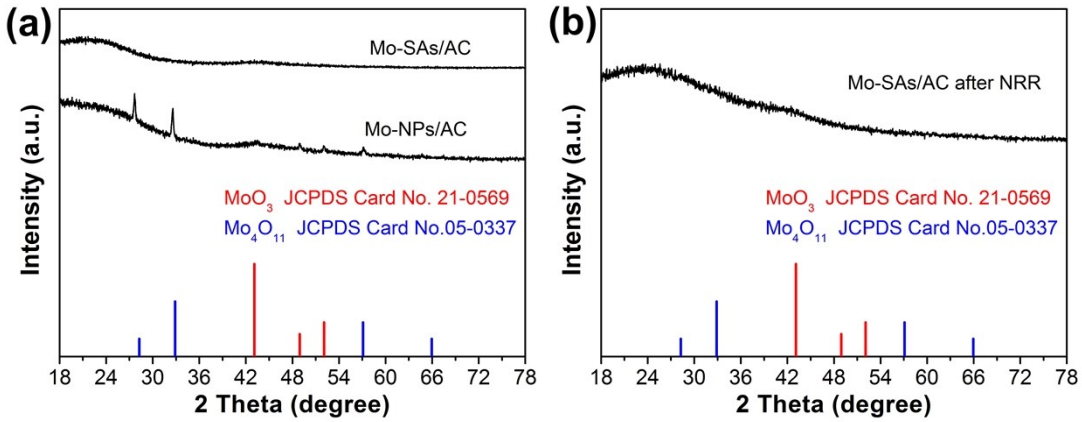

Fig. S3 (a) XRD patterns of Mo-NPs/AC and Mo-SAs/AC. (b) XRD patterns of Mo-SAs/AC after 10 h of NRR.

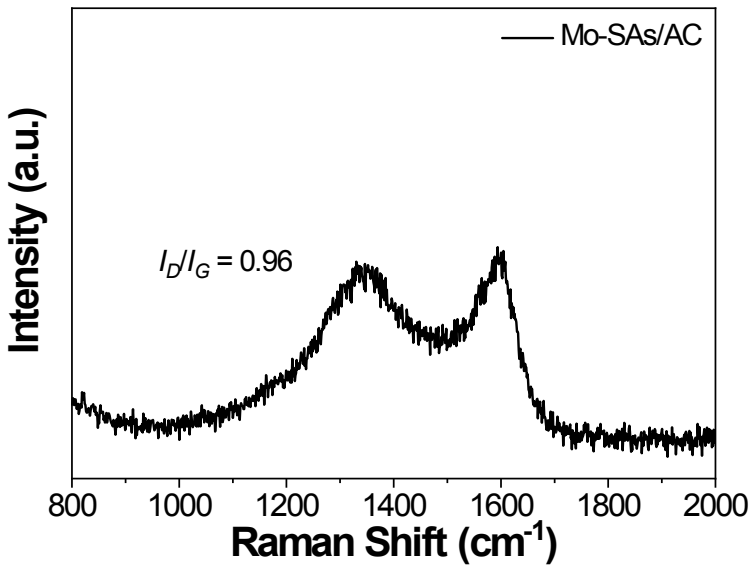

Fig. S4 Raman spectrum of Mo-SAs/AC.

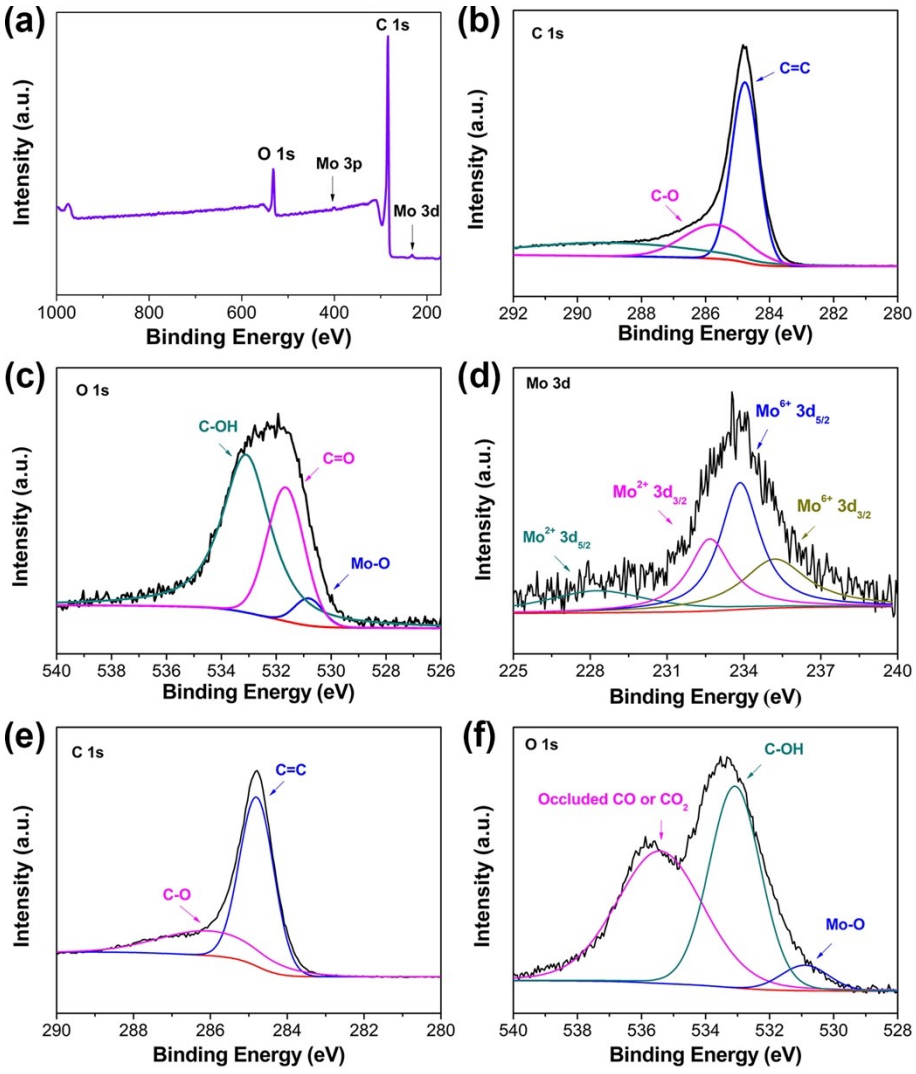

Fig. S5 The surface survey spectrum (a) and XPS spectra of the C 1s (b) and O 1s (c) of Mo-SAs/AC. The corresponding XPS spectra of Mo 3d (d) and C 1s (e) and O 1s (f) of Mo-SAs/AC after 10 h of NRR.

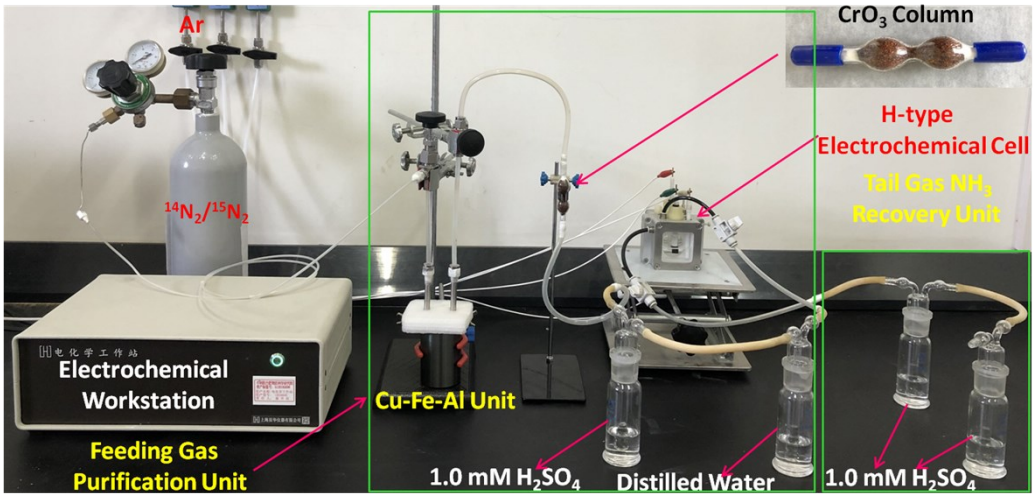

Fig. S6 Photograph of the electrochemical experimental setup including feeding gas purification units.

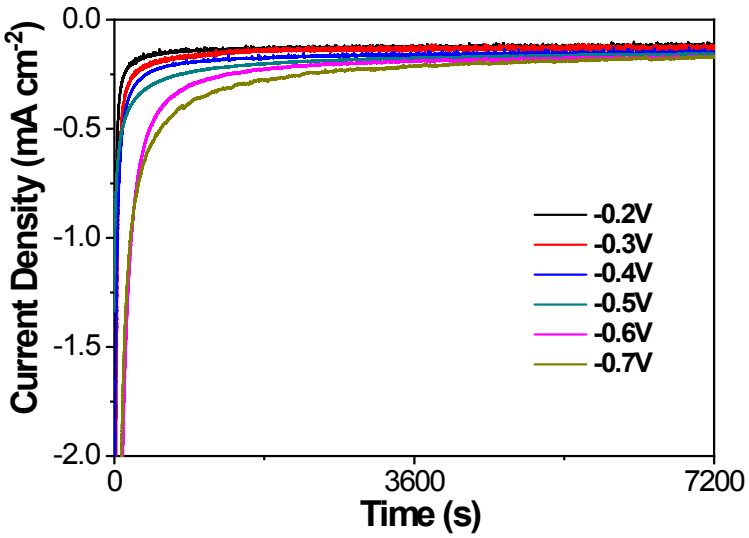

Fig. S7 The *i–t* curves of Mo-SAs/AC for 2 h of NRR at various potentials (*vs.* RHE).

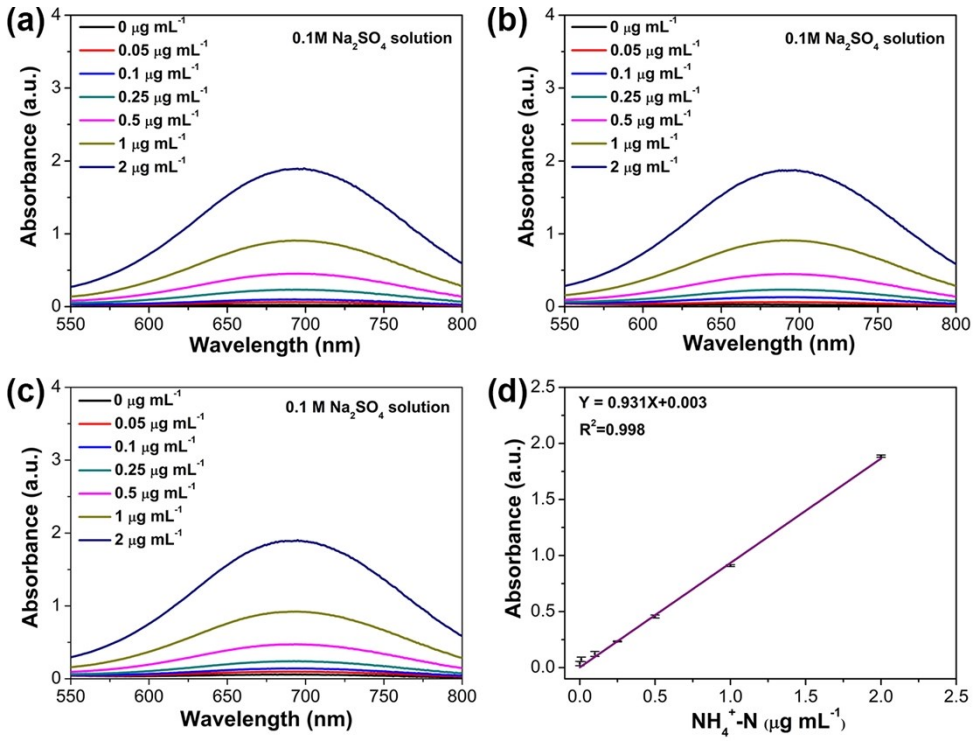

Fig. S8 (a), (b) and (c) UV/Vis absorption spectra of various NH_3 concentrations for three repeated experiments. (d) Calibration curve used for estimation of NH_3 concentration.

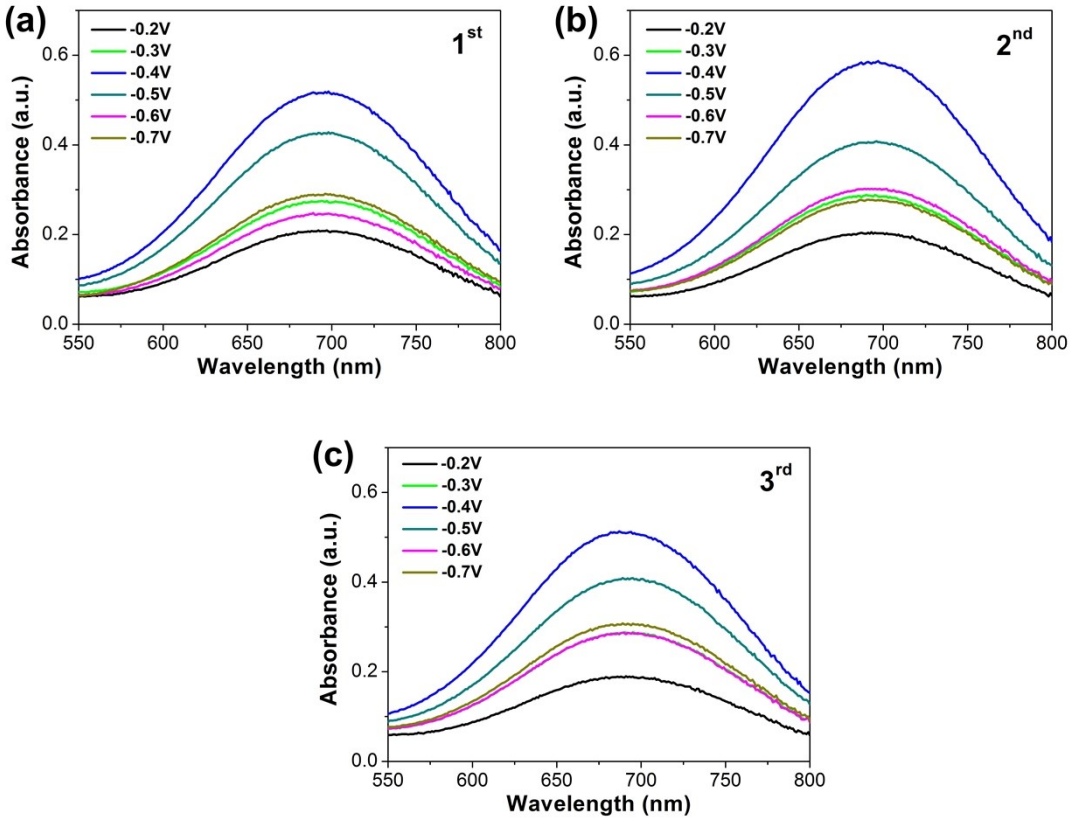

Fig. S9 UV-Vis absorption spectra of electrolytes stained with the indophenol indicator after NRR for 2 h for three repeated experiments.

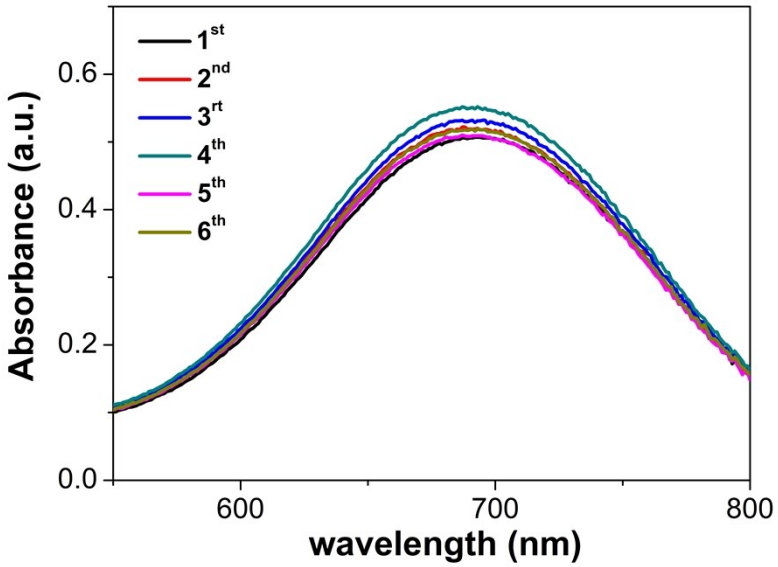

Fig. S10 UV-Vis absorption spectra of electrolytes stained with indophenol indicator for 6 cycles with 2 h NRR period per cycle at –0.40 V *vs.* RHE.

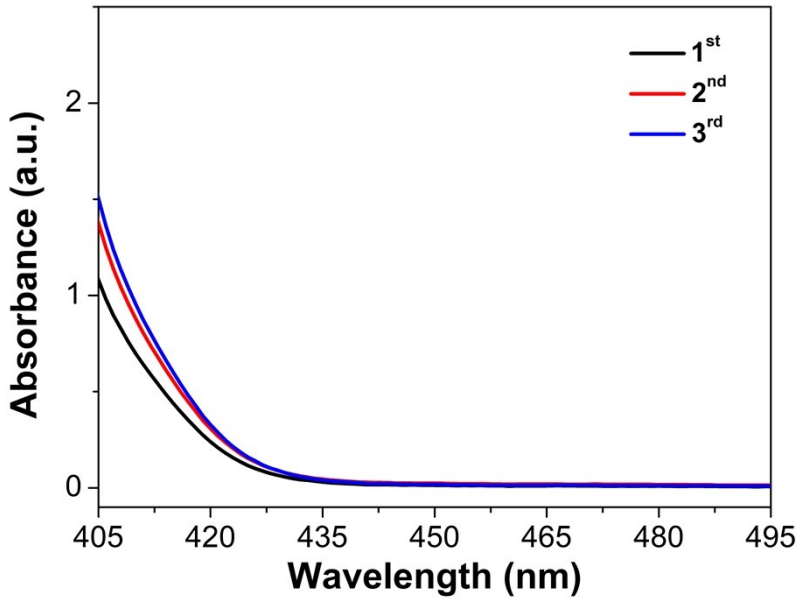

Fig. S11 UV–Vis absorption spectra of the electrolytes measured by the method of Watt and Chrisp after 2h of electrolysis at –0.40 V *vs.* RHE.

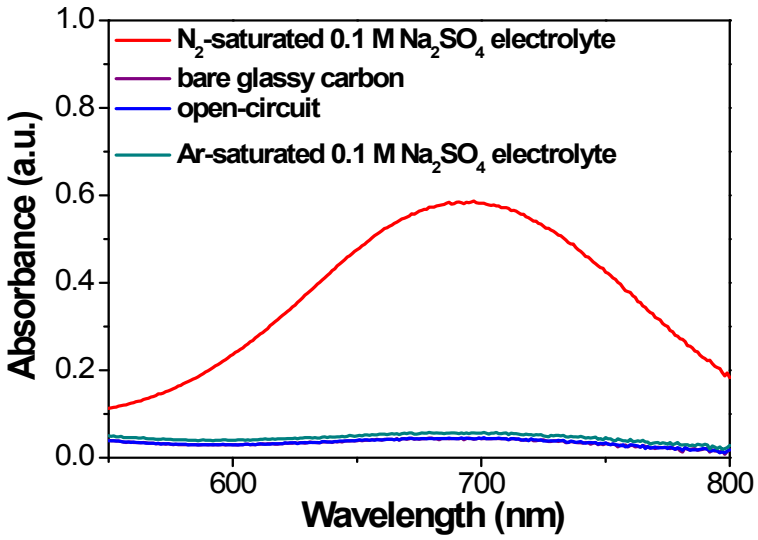

Fig. S12 UV-Vis absorption spectra of the electrolytes obtained under open-circuit, bare glassy carbon and Ar-saturated electrolyte. All solutions were incubated with NH_3 color agent for 1 h before all measurements.

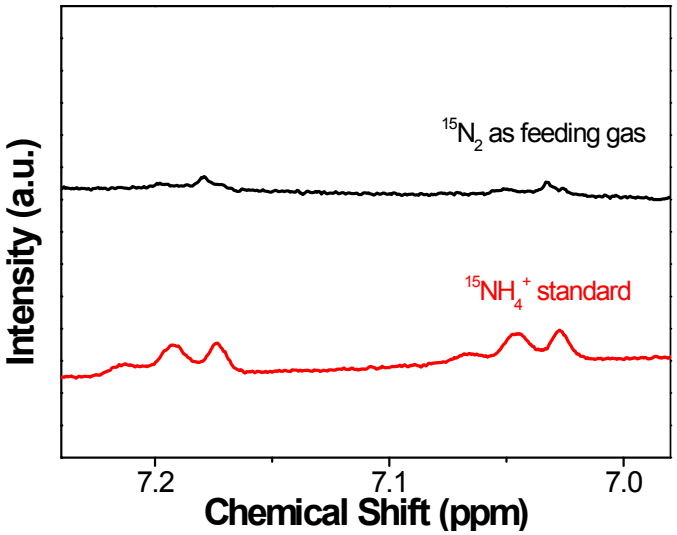

Fig. S13 ^{1}H NMR spectra of NRR samples using $^{15}N_2$ as the feeding gas and standard.

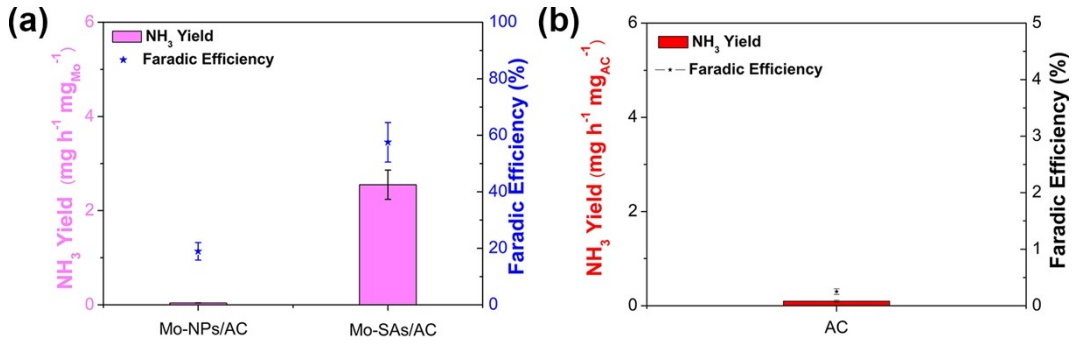

Fig. S14 NH_3 yield rate and FE of Mo-NPs/AC, Mo-SAs/AC (a) and pure AC (b) at -0.40 V (*vs.* RHE) after 2 h of NRR.

References

1. X. Q. Wang, W. Y. Wang, M. Qiao, W. X. Chen, T. W. Yuan, Q. Xu, Min. Chen, Y. Zhang, X. Wang, J. Wang, X . Hong, Y. F. Li, Y. Wu and Y. D. Li, *Sci Bull.,* 2018, **63**, 1246-1253.
2. Z. G. Geng, Y. Liu, X. D. Kong, P. Li, K. Li, Z. Y. Li, J. J. Du, M. Shu, R. Si and J. Zeng, *Adv. Mater.,*2018, **30**, 1803498.
3. H. C. Tao, C. Choi, L. X. Ding, Z. Jiang, Z. S. Hang, M. W. Jia, Q. Fan, Y. N. Gao, H. H. Wang, A. W. Robertson, S. Hong, Y. S. Jun, S. Z. Liu and Z. Y. Sun, *CHEM,* 2019, **5(1)**, 204—214.
4. L. L. Han, X. J. Liu, J. P. Cheng, R. Q. Liu, H. X. Liu, F. Lu, S. Back, Z. X. Liang, S. Z. Zhao, E. Stavitski, J. Luo, R. R. Adzic and H. L. L. Xin, *Angew. Chem. Int. Ed.,* 2019, **58**, 2321-2325.
5. M. F. Wang, S. S. Liu, T. Qian, J. Liu, J. Q. Zhou, H. Q. Ji, J. Xiong, J. Zhong and C. L. Yan, *Nat. Commun.,* 2019, **10**, 341.
6. F. Lu, S. Z. Zhao, R. J. Guo, J. He, S. Y. Peng, H. H. Bao, J. T. Fu, L. L. Han, G. C. Qi, J. Luo, X. L. Tang and X. J. Liu, *Nano Energy,* 2019, **61**, 420-427.
7. W. J. Zang, T. Yang, H. Y. Zou, S. B. Xi, H. Zhang, S. M. Liu, Z. K. Kou, Y. H. Du, Y. P. Feng, L. Shen, L. L. Duan, J. Wang and S. J. Pennycook, ACS Catal., 2019, **9**, 10166-10173.
8. L. Hui, Y. Xue, H. Yu, Y. Liu, Y. Fang, C. Xing, B. Huang and Y. Li, *J. Am. Chem. Soc.,* 2019, **141**, 10677-10683.
9. R. Zhang, L. Jiao, W. J. Yang, G. Wang and H. L. Jiang, *J. Mater. Chem. A*, 2019,**7**, 26371-26377.

10. Y. Liu, Q. Xu, X. Fan, X. Quan and Z. Cai, *J. Mater. Chem. A,* 2019, **7**, 26358-26363.
11. B. Yu, H. Li, J. White, S. Donne, J. B. Yi, S. B. Xi, Y. Fu, G. Henkelman, H. Yu, Z. L. Cheng and T. Y. Ma, *Adv. Funct. Mater.,* 2020, **30**, 1905665.
12. S. B. Zhang, M. Jin, T. F. Shi, M. M. Han, Q. Sun, Y. Lin, Z. H. Ding, L. R. Zheng, G. Z. Wang, Y. X. Zhang, H. M. Zhang, and H. J. Zhao, *Angew. Chem. Int. Ed.*, 2020, **59**, 13423-13429
13. S. Zhang, Q. Jiang, T. Shi, Q. Sun and H. Zhao, *ACS Appl. Energy Mater,* 2020, **3**, 6079-6086.
14. L. L. Zhang, M. Y. Cong, X. Ding, Y. Jin, F. F. Xu, Y. Wang, L. Chen and L. X. Zhang, *Angew. Chem. Int. Ed.,* 2020, **59**, 10888-10893.
15. W. Peng, M. Luo, X. D. Xu, K. Jiang, M. Peng, D. C. Chen, T. S. Chan and Y. W. Tan, *Adv. Energy Mater.*, 2020, **10**, 2001364.
16. J. Li, S. Chen, F. Quan, G. Zhan and L. Zhang, *Chem,* 2020, **6**, 885-901.
17. Y. Y. Ma, T. Yang, H. Y. Zou, W. J. Zang, Z. K. Kou, L. Mao, Y. P. Feng, L. Shen, S. J. Pennycook, L. L. Duan, X. Li and J. Wang, *Adv. Mater.*, 2020, **32**, 2002177.
18. H. Y. Su, L. L. Chen, Y. Z. Chen, R. Si, Y. T. Wu, X. N. Wu, Z. G. Geng, W. H. Zhang and J. Zeng, *Angew. Chem. Int. Ed.,* 2020, **59**, 20411-20416.
19. Y. Chen,R. J. Guo,X. Y. Peng,X. Q. Wang,X. J. Liu,J. Q. Ren,J. He,L. C. Zhuo,J. Q. Sun,Y. F. Liu, Y. E. Wu, J. Luo, *ACS Nano,* 2020, **14**, 6938-6946.
20. H. D. Yu, Y. R. Xue, L. Hui, C. Zhang, Y. Fang, Y. X. Liu, X. Chen, D. Y. Zhang, B. L. Huang, Y. Y. Li, *Nat. Sci. Rev.,* 2020, **nwaa213,** https://doi.org/10.1093/nsr/nwaa213.
21. L. L. Han, M. C. Hou, P. F. Ou, H. Cheng, Z. H. Ren, Z. X. Liang, J. A. Boscoboinik, A. Hunt, I. Waluyo, S. S. Zhang, L. C. Zhuo, J. Song; X. J. Liu, J. Luo, H. L. L. Xin, *ACS Catal.,* 2020, **11**, 509-516.
22. S. Mukherjee, X. X. Yang, W. T. Shan, W. Samarakoon, S. Karakalos, D. A. Cullen, K. More, M. Y. Wang, Z. X. Feng, G. F. Wang, G. Wu, *Small Methods,* 2020, **4**, 1900821.
23. J. Y. Liu, X. Kong, L. R. Zheng, X. Guo,X. F. Liu, J. L. Shui, *ACS Nano,* 2020, **14**, 1093-1101.